

UNIVERSIDAD DE LAS AMÉRICAS PUEBLA

SCHOOL OF SCIENCES

DEPARTMENT OF MATHEMATICS, PHYSICS AND ACTUARIAL SCIENCES



## MAGNETIC PROPERTIES OF INDIUM NITRIDE

MINOR THESIS SUBMITTED BY THE STUDENT

FREDDY ELÍ CAMPILLO DORANTES

159518

ADVISOR

DR. GREGORIO HERNÁNDEZ COCOLETZI



# Contents

<b>1</b>	<b>Introduction</b>	<b>4</b>
<b>2</b>	<b>Density Functional Theory</b>	<b>5</b>
2.1	Electron-electron interactions . . . . .	5
2.1.1	Hohenberg-Kohn theorems . . . . .	6
2.1.2	Kohn-Sham equation . . . . .	6
2.1.3	General method . . . . .	7
2.1.4	Approximations for the exchange-correlation functional: LDA . . . . .	7
2.2	Periodicity and aperiodicity . . . . .	8
2.2.1	Bloch's theorem and plane waves . . . . .	8
2.2.2	Plane wave representation of the Kohn-Sham equations . . . . .	8
2.2.3	Aperiodicity, supercells, and surfaces . . . . .	9
2.3	Ion-electron interactions . . . . .	9
2.3.1	Pseudopotential approximation . . . . .	9
2.4	Ion-ion interactions . . . . .	9
2.5	Broyden-Fletcher-Goldfarb-Shanno algorithm . . . . .	9
<b>3</b>	<b>Computational Method</b>	<b>10</b>
3.1	Construction of the surface . . . . .	10
3.2	Epitaxial growth . . . . .	11
3.3	Surface formation energy . . . . .	12
3.4	Density of states . . . . .	12
<b>4</b>	<b>Results</b>	<b>14</b>
4.1	Adsorption of Mn atoms . . . . .	14
4.2	Mn incorporation . . . . .	15
4.3	Epitaxial growth . . . . .	15
4.4	Surface formation energy . . . . .	16
4.5	Electronic properties . . . . .	16
4.6	Epitaxial growth . . . . .	16
<b>5</b>	<b>Conclusions</b>	<b>19</b>

### Abstract

**Place holder** Initial stages of the epitaxial manganese nitride growth on the (111)-(2×2) indium nitride surface were studied by first-principles calculation within the density functional theory formalism including spin polarisation. The computational calculations were performed using the PWscf program of the quantum espresso suite, where the electro-ion interactions were treated according to a pseudopotential approach and the exchange-correlation energy is modelled using the generalised gradient approximation. First we studied the adsorption of Mn atoms on high symmetry places, varying the coverage from  $\frac{1}{4}$  to a full monolayer. The results showed the T4 site as the most optimal geometry. Then, Mn incorporation was investigated, this occurs when an Mn atom displaces an In atom from the first layer, with the In become the new adatoms to be adsorbed. The results yielded – as the most favourable structure. Electronic properties were determined by performing density of states (DOS) and projected density of states (PDOS) calculations for the most favourable structures (repeated). For all the different test, the DOS is non zero at the Fermi level, indicating they all are metallic.

**Keywords:** Density functional theory, Epitaxial growth, Indium nitride, Manganese Nitride.

# 1 Introduction

In recent years new studies about the structural, electronic, and magnetic properties of transition metal composites have emerged because of their possible applications in the field of spintronics. In this area, it is important to determine the efficient alignment of the electronic spin. One important type of system are the diluted magnetic semiconductors (DMS) that incorporate of transition metals. DMS monolayers with polarized spins allow an injection of polarized electrons into metal-semiconductor interfaces, that is why it is important to know the spin alignment in heterostructures and interfaces. Gallium (Ga), manganese (Mn) and Arsenic (As) ( $\text{Ga}_{1-x}\text{Mn}_x\text{As}$ ) have been investigated because they possess magnetic properties, however, they also have a low Curie temperature. Now, theoretical studies have predicted high curie temperatures for prohibited band gap semiconductors. [2]. Also, first principle studies within the density functional theory have been conducted on MnN in Zinc-blende, sodium chloride and wurzite phases, ignoring spin polarization. [6] Research has been done on MnN and MnAs on Zinc-blende phase where calculations use spin polarization because the materials present magnetic properties, both local density approximations (LDA) and generalized grediente aproximations (GGA) were used.[3] Information relevant of MnN, such as, lattice parameter and bulk modulus have been determined [1], and that it possess stable antiferromagnetic characteristics at temperatures of the order of 753 K [7]. Additionally, first principle studies have been conducted on the stability and the elastic and electronic properties of MnN in tetragonal phase.[8]

In summary, MnN is a transition metal nitride that possesses relevant characteristics for spintronics applications. This material has been well studies in a bulk environment, nevertheless, there's little information about the properties of it's surface configuration. It is our goal to study the epitaxial growth of MnN over the (111) zinc-blende InN surface. This study will explore the possibility that this material could be used as substrate for material growth. The calculations will be performed within the density functional theory including spin polarization using the PWscf program from the quantum espresso suit [4]

## 2 Density Functional Theory

Modelling atomic, molecular or solid systems is a complex and difficult task. There are just a few systems that have complete analytical solutions. It is true that we could obtain useful information using workarounds and approximations, such as perturbation theory, for more difficult, yet small systems. Nevertheless, for most problems of interest, and their corresponding applications, models are constructed with dozen or hundreds of atoms, and here a computational method is required.

It is known that most properties of a given system can be obtained using just total energies and differences in total energies. For example, for the case of a solid, from total energy calculations (and it's subsequent minimisation with respect to the nuclear coordinates) properties like lattice constant, bulk moduli, phonos, pizelectric constant, phase-transitions pressures and temperatures could be obtained. There exist plethora of energy calculations theories and algorithms. Nevertheless, the density functional theory (DFT) was chosen for performing all calculations, as it is optimised for periodic systems. In the following sections, the basic of the theory, requirements and approximations used will be explained.

This theory's first approach to convert this problem in a more manageable one is to use the Born-Openheimer approximation. It states that because the nuclei are many times more massive than the electrons, the electrons respond instantaneously to any modifications on the coordinates of the nuclei. This statement allows us to separate electronic and nuclear coordinates. To solve and electronic problem for a given frozen arrangement of the ions.

For that reason, it is convenient to divide the overall method in four parts, as follows:

1. Electron electron interactions: treated within the DFT theory
2. Periodic and aperiodic systems: usage of a plane waves basis sets and supercells.
3. Ion-electron interaction: Modelled using a pseudo potential approach.
4. Ion-ion interactions

### 2.1 Electron-electron interactions

Most of the computational time in a total energy calculation will be spend in determining the energy contributions of the electron interactions. Firstly, thinking of electrons as charged particles, one would think the only contribution of these to the Hamiltonian would be their respective kinetic energy and a classical Coulomb repulsion. Nevertheless, the nature of electrons that must

obey certain rules under our system allow us to define two more special interactions that have a significant contribution to the total energy: *exchange* and *correlation*.

- **Exchange energy** As electrons obey the Pauli exclusion principle pawns from the anti-symmetric properties of the wave functions of the electrons (since they are fermions). The antisymmetry causes a spatial separation for electrons of the same spin, and this behaviour reduces the total energy. The acknowledgment of this interaction in the calculation is often referred as a Hartree-Fock approximation. Properly defined as:

$$E_x = - \int \psi_i(r) \psi_j(r') \frac{1}{|r - r'|} \psi_i(r) \psi_j(r') dr dr'$$

- **Correlation energy:** the total energy can be reduced once again if *opposite* spin electrons are also spatially separated. This difference is called *correlation energy* and it has proved to be difficult to calculate. Usually defined as the difference between the HF approximation and the exact quantum energy:

$$E_c = E_{tot} - E_{HF}$$

### 2.1.1 Hohenberg-Kohn theorems

Hohenberg and Kohn in 1964 [5] proved formally that the whole system (including exchange and correlation energies) can be described in terms of the electron density ( $n$ ) their article, they state the following theorems:

**Theorem 1.** *The total energy is an unique functional of the electron density  $n(r)$ .*

**Theorem 2.** *The ground state energy can be obtained variationally: the density that minimises the total energy is the exact ground state density.*

### 2.1.2 Kohn-Sham equation

In 1965, W. Kohn and L. J. Sham showed that we could change the many electron problem to an equivalent set of self consistent one electron equations.

The shape of the kohn-sham energy functional is

$$E[\psi_i] = 2 \sum_i \int \psi_i \left[ -\frac{\hbar^2}{2m} \right] \nabla^2 \psi_i dr + \int V_{ion}(r) n(r) d^3r + \frac{e^2}{2} \int \frac{n(r)n(r')}{|r - r'|} d^3r dr' + E_{XC}[n(r)] + E_{ion}(\{R_i\}). \quad (2.1)$$

Where the electron density is defined as:

$$n(r) \equiv 2 \sum_i |\psi_i(r)|^2 \quad (2.2)$$

The equations that minimise this functional, are the self consistent solutions of the Kohn-Sham equations:

$$\epsilon_i \psi_i(\mathbf{r}) = \left[ -\frac{\hbar^2}{2m} \nabla^2 + V_{ion}(r) + V_H(\mathbf{r}) + V_{XC}(\mathbf{r}) \right] \psi_i(\mathbf{r}). \quad (2.3)$$

where  $\psi_i$  is the corresponding wave function of the electronic states  $i$  and  $\epsilon_i$  is the KS eigenvalue.  $V_H$  is the Hartree potential, given by:

$$V_H(\mathbf{r}) = e^2 \int \frac{n(\mathbf{r}')}{|\mathbf{r} - \mathbf{r}'|} d^3\mathbf{r}' \quad (2.4)$$

. The exchange-correlation functional  $y$  given by the functional derivative of the exchange-correlation energy.

$$V_{XC}(\mathbf{r}) = \frac{\delta E[n(\mathbf{r})]}{\delta n(\mathbf{r})} \quad (2.5)$$

### 2.1.3 General method

In order to solve the Kohn-Sham equations, the method need a trial electron density as a starting point. With it one can solve the KS-equations and find the electron wave functions. According to equation 2.2, one can easily calculate a new, and improved, electron density. One can compare the energies corresponding to each electron density. If the difference between them is less than a certain tolerance, then the ground state was found; if it is larger, the new electron density becomes the trial one, and the cycle continues until convergence is achieved.

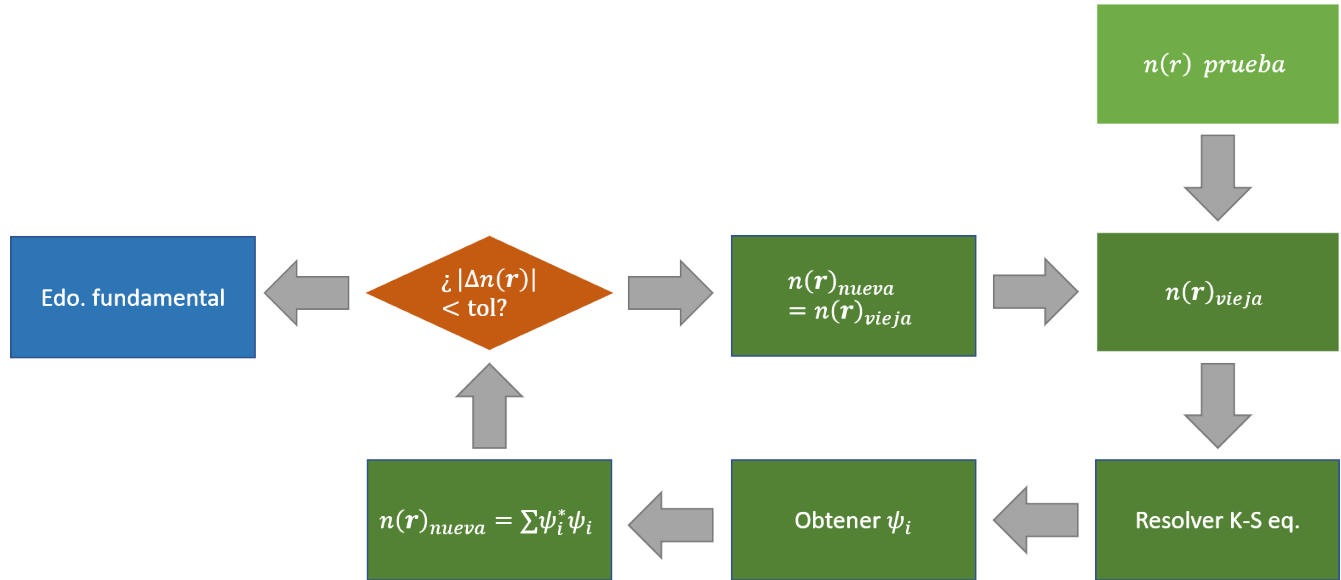


Figure 2.1: Representation of the self-consistent process for solving Kohn-Sham equations.

### 2.1.4 Approximations for the exchange-correlation functional: LDA

One of the simplest method for approximate the exchange-correlation energy is a method called the *local density approximation* or LDA. It states that the exchange correlation energy per electron at a point  $r$  of an electron gas is equal to the exchange-correlation energy per electron in a **homogeneous** gas that has the same density at the point  $r$ .

$$E_{XC}[n(r)] = \int \epsilon_{XC} n(\mathbf{r}) d^3\mathbf{r} \quad (2.6)$$



$$\frac{\delta E[n(\mathbf{r})]}{\delta n(\mathbf{r})} = \frac{\delta E[n(\mathbf{r})\epsilon_{XC}(\mathbf{r})]}{\delta n(\mathbf{r})} \quad (2.7)$$

$$\epsilon_{XC}(\mathbf{r}) = \epsilon^{hom} XC(\mathbf{r}) \quad (2.8)$$

## 2.2 Periodicity and aperiodicity

### 2.2.1 Bloch's theorem and plane waves

From a theoretical background in solid state physics we know that we can approach a periodic system, by solving the problem in it's Wigner Seitz cell, or the minimum unit of repetition, utilizing the appropriated boundary conditions.

Bloch's theorem states that the electron wave function in a periodic solid is the product of a wave-like part and a cell periodic part ( $f_i$ ). The first of them can be written in exponential form, a plane wave, dependent of the vectors in real space.

$$\psi_i(\mathbf{r}) = e^{i\mathbf{k}\cdot\mathbf{r}} f_i(\mathbf{r}) \quad (2.9)$$

Then, the cell periodic part can be expanded in a basis of plane waves whose wave vectors are the reciprocal lattice vectors.

$$f_i(\mathbf{r}) = \sum_i c_{i,G} e^{i\mathbf{G}\cdot\mathbf{r}} \quad (2.10)$$

The reciprocal lattice vectors are related to the regular lattice vectors ( $\mathbf{l}$ ) by the following equation.  $\mathbf{G} \cdot \mathbf{l} = 2m\pi$  where  $m$  is an integer. Therefore, the electron wave function can be expanded in a basis of discrete plane waves as:

$$\psi_i(\mathbf{r}) = \sum_G c_{i,\mathbf{k}+\mathbf{G}} e^{i\mathbf{k}\cdot\mathbf{r}} \quad (2.11)$$

In principle, this basis set is infinite. However, the coefficients of the waves with small kinetic energy are generally more important. For that reason it is convenient to truncate the basis set at an arbitrary energy, called **cutoff energy**. This combined with the fact that the plane waves are discrete (not continuous) make the problem capable to be performed computationally.

Naturally, this truncation makes our result not exact. A large cutoff energy would make the error smaller, and our result more precise, at a cost of computational power or more time.

### 2.2.2 Plane wave representation of the Kohn-Sham equations

One other advantage of working with a basis of plane waves is that the KS-equations acquire a simpler form. By combination of equations 2.11 and 2.3, we can obtain the following equivalent

equations.

$$\sum_{\mathbf{G}'} \left[ -\frac{\hbar^2}{2m} |\mathbf{k} + \mathbf{G}|^2 \delta_{\mathbf{G}\mathbf{G}'} + V_{ion}(\mathbf{G} - \mathbf{G}') + V_H(\mathbf{G} - \mathbf{G}') + V_{XC}(\mathbf{G} - \mathbf{G}') \right] c_{i,\mathbf{k}+\mathbf{G}'} = \epsilon_i c_{i,(\mathbf{k}+\mathbf{G})} \quad (2.12)$$

### 2.2.3 Aperiodicity, supercells, and surfaces

Bloch theorem can not be used in non periodic systems. Examples are crystals that contain defects or in the direction perpendicular to a surface. An infinite number of plane waves would be required for modelling those kinds of systems. The only solution that avoids this problem is to make use of a supercell. A supercell becomes the new unit that will be repeated through space. Inside it we can model the defect surrounded by a bulk of crystal, the approximation will be better if we increase the size of the supercell until it converges.

One can construct supercells to treat problems like surfaces or even single molecules in a similar manner.

## 2.3 Ion-electron interactions

### 2.3.1 Pseudopotential approximation

## 2.4 Ion-ion interactions

## 2.5 Broyden–Fletcher–Goldfarb–Shanno algorithm

BFGS quasi-newton algorithm, based on the trust radius procedure, for structural relaxation

## 3 Computational Method

All calculations were performed within the density functional theory as implemented in the PWscf program of the quantum espresso suite. The exchange-correlation potential energies were treated according to the generalized gradient approximation (GGA) with the Perdew, Burke, Ernzerhof (PBE) gradient corrected functional. The electron-ion interactions were treated according to the pseudopotential approach, employing Vanderbilt ultrasoft pseudopotentials. Electron states are expanded in plane waves with an energy cut off of 40 Ry and a charge density cut off of 320 Ry. For the optimisation, all the forces must be smaller than 0.026 eV/Å and the energy difference should be less than 0.0014.

### 3.1 Construction of the surface

To precise, the aim of this work is to investigate the initial stages of the MnN growth on the InN (1 1 1) surface. As previously discussed, a supercell approach is required to treat aperiodic systems such as surfaces. For its construction, the optimal lattice parameter of the indium nitride crystal in a zinc-blende phase was determined by performing total energy calculations using a  $(5 \times 5 \times 5)$  mesh to sample the Brillouin zone. Then, the In-terminated supercell of the (111) surface was constructed with a slab of 4 InN bilayers of  $(2 \times 2)$  periodicity and a vacuum gap of  $\approx 15.8$  Å to ensure a separation of at least 10 Å for every future calculation. The supercell is constructed with dimensions equivalent to the optimised bulk lattice parameter. The bottom InN bilayer is saturated with pseudo hydrogen atoms to simulate a bulk like environment.

Studies consider the adsorption, incorporation and diffusion of Mn into the structure. A schematic representation of the InN (1 1 1)- $(2 \times 2)$  surface is shown in Fig. 3.3, the top view is at the left side and the side view is at the right. This phenomena are most likely to occur at high symmetry sites on the surface, consequently calculations only consider three of them (H3, T4 and Top) indicated in Fig. 3.3 a.

The  $(2 \times 2)$  periodicity of the cell allows to vary the coverage of the atoms, from  $\frac{1}{4}$  to a full monolayer of Mn. As Mn atoms are magnetic, different calculations are needed for the non magnetic, ferromagnetic and antiferromagnetic configurations, as long as the number of Mn atoms in the structure allows it.

#### High symmetry sites for adsorption of Mn atoms

The adsorption of Mn atoms consist on placing Mn atoms on one of the specific high symmetry points discussed before. In the H3 site the Mn adatom bonds to three N atoms of the first monolayer (ML) above a nitrogen atom of the fourth monolayer. In the T4 site the Mn adatom

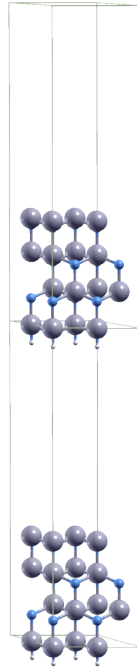


Figure 3.1: Diagram of the implementation of the supercell. The empty space ensures we are treating a surface while retaining continuity and periodicity in the x and y directions.

bonds to three In atoms of the first monolayer above nitrogen atoms of the second monolayer. And the Top site is obtained when the Mn atoms are placed on top of the In atoms of the first ML.

### High symmetry sites for incorporation of Mn atoms

The Mn incorporation into the InN  $(1 \times 1)-(2 \times 2)$  surface occurs when a Mn atom displaces an InN atom of the first ML, then the displaced InN atom transforms into the new adatom.

An observant reader can quickly notice that this experiment is not as simple as the adsorption, since the symmetry of the surface is lost in this process. When the adsorption of the In adatom occurs we can notice that not all symmetry sites are equal for these atoms could interact only with other In atoms or with In and Mn atoms. This generates two sets of high symmetry sites. Named, for convenience 1 and 2. A schematic for these sites is represented in Fig. 3.4

**Set1** In the first kind, the In adatom interacts with Mn and In atoms of the first ML (H3-1, T4-1, Top-1 and Bridge-1), while in the

**Set2** while in the second kind, the In ad-atom forms bonds with In atoms only (H3-2, T4-2, Top-2 and Bridge-2), these high symmetry sites are displayed in

## 3.2 Epitaxial growth

To simulate the first steps of epitaxial growth of MnN on the InN surface, total energy calculation must be performed on new systems. This time, up to two bilayers of MnN are placed on top of the clean surface system. In this process, we have to be mindful that for each bilayer, the

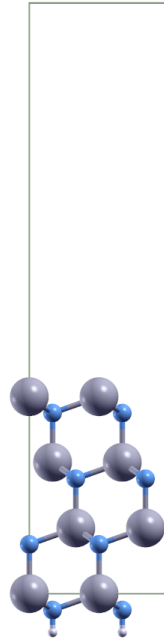


Figure 3.2: Placeholder for supercell image, mine but incomplete

corresponding Mn monolayer could be placed where a In monolayer would be if we were to extend the surface for 5 In bilayers; or it could be placed in other high symmetry site. In summary, for each new bilayer, the possibility of a H3 or T4 Mn monolayer has to be explored.

### 3.3 Surface formation energy

For this calculation the energies of individual atoms of In, N and Mn are needed. Those are obtained from the energy optimisation of basis structures consisting of only one of these atoms. The chosen structures are: cubic In, molecular nitrogen ( $N_2$ ), and crystal manganese in an alpha configuration. Once these energies are obtained, the surface formation energy for a selection of the most favourable structures with respect to the clean surface is obtained, in both N and In rich conditions.

### 3.4 Density of states

Finally, for the analysis of the electronic properties of the chosen structures, calculations of the density of states and projected density of states must be performed, using the programs *dos* and *pdos* from the quantum espresso suite.

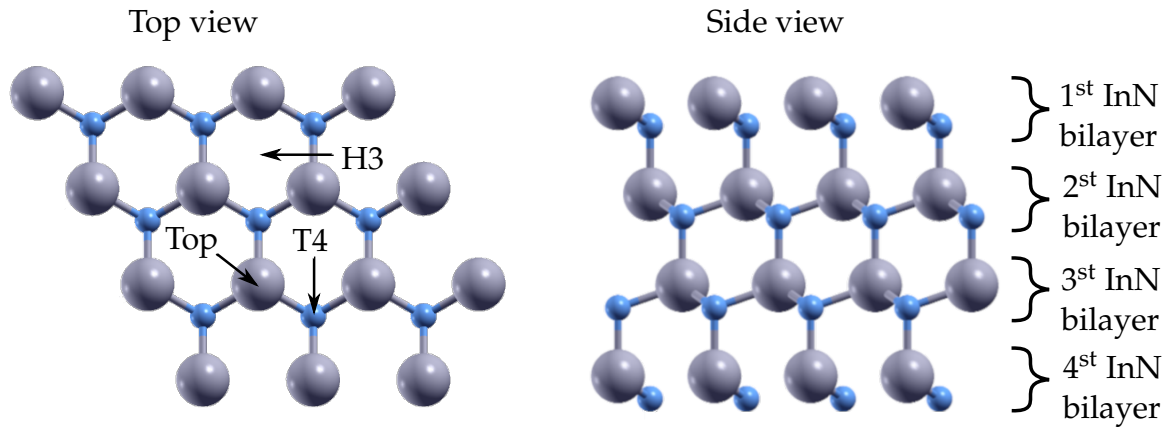


Figure 3.3: Schematics for the atomic structures of the In terminated InN (111)-( $2 \times 2$ ) surface. The high symmetry sites T4, H3 and top are shown. Left, top view; right, side view.

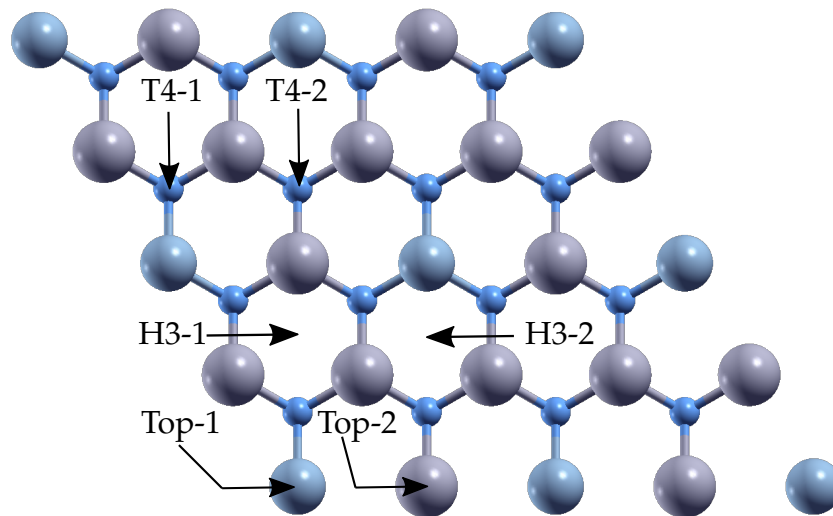


Figure 3.4: Schematic representation of the two sets of high symmetry places that incorporation allows sites named -1 mean that that adatoms connect to to Mn atoms -2 means only bonds to another In atoms.

## 4 Results

### 4.1 Adsorption of Mn atoms

In table 4.1 the relative energies resulting from the absorption of Mn at different coverage is shown. The configuration of reference is the ferromagnetic T4 site for all cases, at it is the most stable configuration. For the different sites, for all configuration follows this relation: Top < H3 < T4. While, for all sites the non magnetic case exhibits the highest energy. For sites H3 and Top, the antiferromagnetic config is the most stable for 1/4 and 3/4 ML, while is is the antiferromagnetic case for the 1/2 ML and 1 ML cases.

$\frac{1}{4}$ Mn ML			$\frac{1}{2}$ Mn ML			$\frac{3}{4}$ Mn ML			1 Mn ML					
Site	Energy (eV)		Site	Energy (eV)			Site	Energy (eV)			Site	Energy (eV)		
	NM	FM		NM	FM	AFM		NM	FM	AFM		NM	FM	AFM
T4	0.447	0.000	T4	1.471	0.000	0.033	T4	2.704	0.000	0.041	T4	8.923	0.067	0.000
H3	2.294	0.025	H3	5.317	0.386	0.368	H3	3.240	0.343	0.413	H3	10.345	0.715	0.584
Top	3.884	1.062	Top	6.822	1.424	1.410	Top	3.594	1.465	1.275	Top	11.753	1.812	1.515

Table 4.1: Relative energies in eV for different coverages of the Mn absorption. Reference is the T4 site for each coverage.

As stated in before, the Mn incorporation spawns two sets of symmetry sites. For the first set the most stable site changes from t4 for 1/4 ML to H3 for 1/2 and 3/4 ML to T4 again at a ful ML. In all cases excep the first the prefered states is the antiferromagnetic configuration, for 1/4 ML it is ferromagnetic.

## 4.2 Mn incorporation

### Set 1

$\frac{1}{4}$ Mn ML			$\frac{1}{2}$ Mn ML				$\frac{3}{4}$ Mn ML				1 Mn ML			
Site	Energy (eV)		Site	Energy (eV)			Site	Energy (eV)			Site	Energy (eV)		
	NM	FM		NM	FM	AFM		NM	FM	AFM		NM	FM	AFM
T4-1	-1.993	-2.204	T4-1	-3.597	-3.774	-3.823	T4-1	-2.469	-4.472	-4.556	T4-1	-1.958	-6.630	-6.852
H3-1	-1.847	-2.019	H3-1	-3.102	-3.837	-3.888	H3-1	-3.346	-4.253	-4.668	H3-1	-1.769	-6.169	-6.328
Top-1	-1.529	-1.695	Top-1	-3.036	-3.661	-3.482	Top-1	-2.553	-4.048	-4.029	Top-1	-1.020	-5.658	-5.638

Table 4.2: Relative energies for the different coverages of the Mn incorporation for set 1 of the high symmetry sites. Reference is the most stable incorporation for each coverage.

### Set 2

$\frac{1}{4}$ Mn ML			$\frac{1}{2}$ Mn ML			$\frac{3}{4}$ Mn ML			1 Mn ML					
Site	Energy (eV)		Site	Energy (eV)			Site	Energy (eV)			Site	Energy (eV)		
	NM	FM		NM	FM	AFM		NM	FM	AFM		NM	FM	AFM
T4-2	0.000	0.000	T4-2	0.000	0.000	0.000	T4-2	0.000	0.000	0.000	T4	0.000	0.000	0.000
H3-2	0.000	0.000	H3-2	0.000	0.000	0.000	H3-2	0.000	0.000	0.000	H3	0.000	0.000	0.000
Top-2	0.000	0.000	Top-2	0.000	0.000	0.000	Top-2	0.000	0.000	0.000	top	0.000	0.000	0.000

Table 4.3: Relative energies for the different coverages of the Mn incorporation for set 2 of the high symmetry sites. Reference is the most stable incorporation for each coverage.

## 4.3 Epitaxial growth

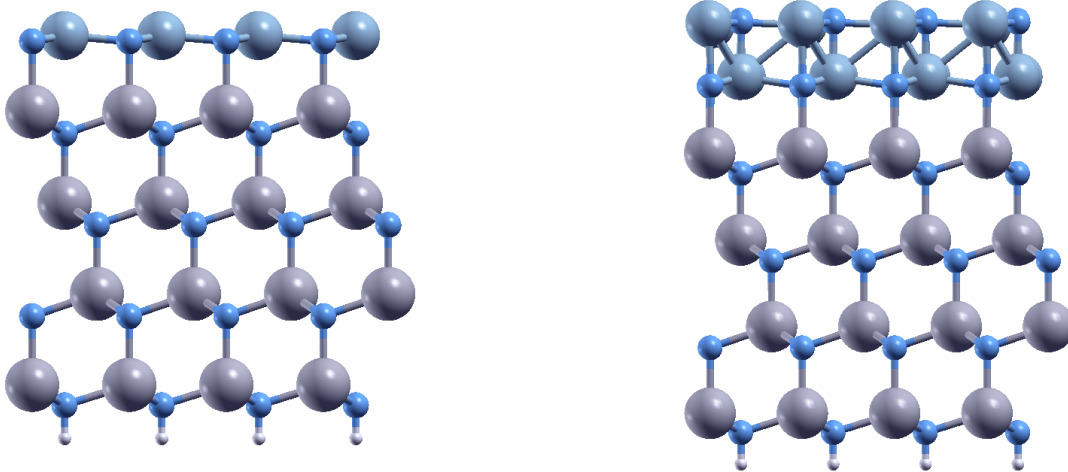


Figure 4.1: Modelling of the first steps of Mn growth on the InN (111) surface. 1 MnN bilayer (left) and 2 MnN bilayers (right) systems were studied.



## 4.4 Surface formation energy

For this calculation the energies of individual atoms of In, N and Mn are needed. Those are obtained from the energy optimisation of basis structures consisting of only one of these atoms. The chosen structures are: cubic In, molecular nitrogen (N<sub>2</sub>), and crystal manganese in an alpha configuration. Once these energies are obtained, the surface formation energy for a selection of the most favourable structures with respect to the clean surface is obtained, in both N and In rich conditions.

## 4.5 Electronic properties

Finally, for the analysis of the electronic properties of the chosen most stable structures. Calculations of the density of states and projected density of states are plotted as functions of energy, using the fermi level as reference.

Figure 4.2 represents the clean (111) InN surface. The black line represents the results from the DOS calculations, as there is no energy gap at the Fermi level, which indicated that the In-terminated surface is a material of metallic behaviour. The PDOS calculations are shown in the rest of the figure, only the *p* orbitals for the Nitrogen (red) and Indium (blue) indicate that the metallicity of this structure is only due to the first bilayer.

## 4.6 Epitaxial growth

**Surface formation energy**

**Density of states**

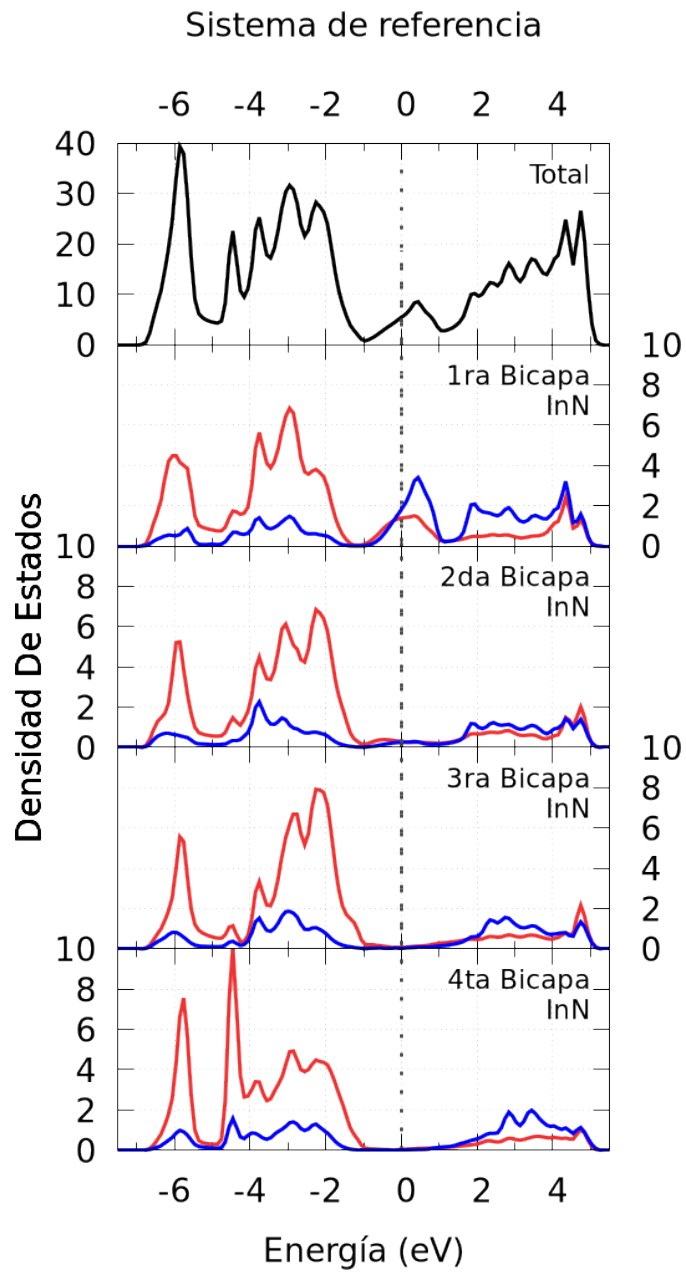


Figure 4.2: Density of states and projected density of states for the reference system. The first graph (black line) shows the total DOS. The following graphs exhibit the PDOS for the first, second, third and fourth InN bilayers, respectively. Only the  $p$  orbitals were considered for N (red) and In (blue) atoms.

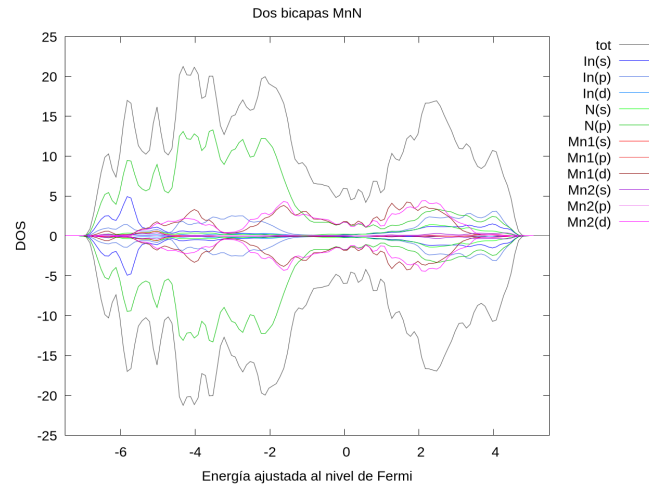


Figure 4.3: Density of states and projected density of states for an antiferromagnetic system of two MnN bilayers.

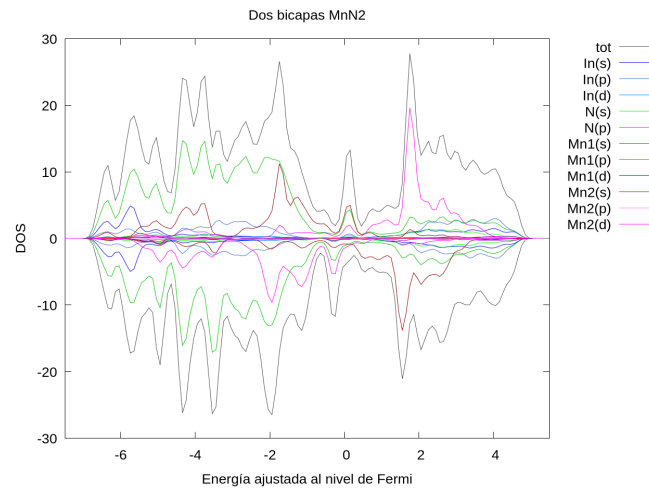


Figure 4.4: Density of states and projected density of states for an antiferromagnetic system of two MnN bilayers at a different spin configuration.

## 5 Conclusions

# Bibliography

- [1] Li Cheng-Bin et al. "First principles study on the charge density and the bulk modulus of the transition metals and their carbides and nitrides". In: *Chinese Physics* 14.11 (2005), p. 2287.
- [2] T Dietl, o H Ohno, and F Matsukura. "Hole-mediated ferromagnetism in tetrahedrally coordinated semiconductors". In: *Physical Review B* 63.19 (2001), p. 195205.
- [3] R Espitia, JH Díaz, and OJ Salcedo. "Computational Calculation of the Relative Phase of the MnN Compound". In: *International Journal of Mathematical Análisis* 11 (2017), pp. 1081–1088.
- [4] Paolo Giannozzi et al. "QUANTUM ESPRESSO: a modular and open-source software project for quantum simulations of materials". In: *Journal of physics: Condensed matter* 21.39 (2009), p. 395502.
- [5] Pierre Hohenberg and Walter Kohn. "Inhomogeneous electron gas". In: *Physical review* 136.3B (1964), B864.
- [6] R de Paiva et al. "First-principles materials study for spintronics: MnAs and MnN". In: *Brazilian Journal of Physics* 34 (2004), pp. 568–570.
- [7] K Suzuki et al. "Crystal structure and magnetic properties of the compound MnN". In: *Journal of alloys and compounds* 306.1-2 (2000), pp. 66–71.
- [8] Ran Yu et al. "The stability, electronic structure, elastic and metallic properties of manganese nitrides". In: *RSC advances* 5.2 (2015), pp. 1620–1627.